

Explosive nucleosynthesis, equilibrium thermodynamics, and relativistic heavy-ion collisions

A. Z. Mekjian

*Nuclear Science Division, Lawrence Berkeley Laboratory, University of California, Berkeley, California 94720
and Department of Physics, Rutgers University, New Brunswick, New Jersey 08903*

(Received 18 July 1977)

A description of the formation of composite nuclei observed in relativistic heavy-ion collisions is developed. The description is analogous to that used in accounting for the formation of nuclei under explosive conditions, as encountered in the expansion of an isotropic and homogeneous universe and in imploding-exploding supermassive stars. The model studied is one in which composite nuclei are formed in the space-time evolution of a rapidly expanding system of nucleons. Within the framework of this model, it is shown that reaction rates may initially be fast compared to expansion time scales, that detailed balance can then be met and a quasiequilibrium established for a short period of time and limited volume of space in this space-time evolution. An idealized equilibrium model is then proposed which contains a sharp cutoff from equilibrium to free expansion. In such a model the observed properties of the composite particles reflect a "frozen in" equilibrium state. A simple discussion is then presented showing that the volume at which the transition occurs is related to the finite size of the correlated structures in the system. A key result in the approach developed is that properties of the composite particle cross sections can be used to obtain information on the size of the emitting region without resorting to a Hanbury-Brown-Twiss correlation measurement. Another important result is that cross sections for composite nuclei are characterized by Maxwell-Boltzmann distributions in some rest system and recent data will be discussed from this viewpoint. The thermodynamic properties of the system, such as the equation of state and the energy-temperature relationship are investigated. The effect of continuum correlations from resonances and echoes will also be discussed.

[NUCLEAR REACTIONS Thermodynamic model of heavy-ion collisions at relativistic energies. Theory of formation of composite nuclei in space-time evolution of an expanding system of nucleons.]

I. INTRODUCTION

In heavy-ion collisions at relativistic energies, events are observed in streamer chamber experiments¹⁻³ which are quite violent or explosive. High energy fragments are seen over most of the forward hemisphere with velocities intermediate between the incident projectile velocity (with superimposed Fermi velocity) and the Fermi motion of the target. Some events show multiplicities exceeding one hundred charged particles whose transverse momenta are quite high. These events are associated with near central collisions.⁴⁻⁶ By contrast, peripheral collisions show a quite different but more familiar cosmic-ray-like pattern. Specifically, they show a star from target evaporation which is isotropic and a narrow jet from projectile fragmentation whose longitudinal momenta are near to the beam momenta and whose transverse momenta are small.

In another series of experiments,⁵⁻⁷ inclusive spectra of protons, deuterons, tritons, and helium nuclei were measured at large angles and intermediate energies in the hope of investigating properties of the more central collisions. Heavier fragments up to oxygen have also been reported.^{5,8}

The objective of such experiments is to supply information for studies of nuclear matter at temperatures and densities far from normal nuclei which can occur in the more central collisions.^{4,9} The present paper is an attempt to study some of these features within the framework of a specific model.

For example, an accounting of the number of composite particles, their energy and angular distributions, and the possible correlations they may have contains such information. In an attempt to account for some of these features, a thermodynamic model has already been proposed and its predictions briefly discussed.¹⁰ Here, a sequel to this former study is developed.

The viewpoint to be taken in this endeavor is that the description of the formation of deuterons, tritons, helium nuclei, etc., can be made within a framework that is analogous to that used in describing the formation of the elements under explosive conditions, such as are encountered in the expansion of the universe (big bang model) and in imploding-exploding supermassive stars.^{12,13} The corresponding parallel picture will then be one in which composite nuclei are formed in the space-time evolution of a rapidly expanding system of nucleons which is raised to a high temperature and density.

Of course, the physical conditions in temperature and density are so very different in the environment generated in relativistic heavy-ion collisions that the formation of composite nuclei occurs approximately 10^{23} – 10^{25} times faster here than in the other two situations. But expansion time scales are also correspondingly much shorter so that the descriptions for the formation of composite nuclei in the three cases may be linked by simple scale changes in an established mathematical framework. However, it is shown that the scale change in position (or density) is not compensated by the scale change in time so that the details of the reactions are quite different and that only the structure of the description is left as the common element.

The outline of the paper is as follows. The first major section is devoted to a discussion of the model. In this section the dynamical basis of the model is developed. Expansion time scales and reaction rates are compared and the dynamical process behind the formation of composite particles is studied. From this information an equilibrium model is proposed. The second major section contains the predictions of this equilibrium model in its simplest version. First, the nature of the model is discussed and the Gibbs grand canonical partition function is evaluated. Secondly, the law of mass action is used to obtain the concentrations of nuclei in the thermodynamic region. The observed spectrum of composite nuclei is then discussed. Next, the space-time structure of the emitting region is studied and the size of this region is estimated. A comparison is then made with a final state interaction model of composite particle formation. The remaining subsections are devoted to the other thermodynamic variables and the virial expansion for the equation of state. The third major section is concerned with nuclear resonances and continuum correlations and their effect on the thermodynamic properties of the system. A summary of the paper is then given. Finally, the Appendix summarizes the thermodynamic expressions with the effects of relativity and statistics included.

II. MODEL—QUALITATIVE CONSIDERATIONS AND ITS DYNAMICAL BASIS

A. Preliminary remarks

The collision of two heavy nuclei at high energies has been pictured as follows.^{4,6,14} In a collision of two such nuclei, a division into three regions might be produced which involves “participants” and “spectators.” The participants are those nucleons in the target and projectile which are directly in each others’ path. This region is expected to be

heated to a high temperature and may involve, initially, a high density.^{4,9} The spectators are those nucleons in the target and projectile which do not overlap. They would produce the cosmic-ray-like jet (projectile spectators) and the target star (target spectators). The participant region has been called the nuclear fireball.⁶

Moreover, this qualitative discussion has been taken seriously and a macroscopic model has been developed around it.⁶ In this model, nucleons, mutually swept up in a clean geometrical cut, form a combined system whose excitation energy E^* and collective center of mass motion are obtained from simple kinematics. This inelastic energy then goes into raising the temperature of the nucleons, resulting in a quasiequilibrated fireball with a Boltzmann distribution of velocities for the nucleons. From the number of nucleons in the fireball, its temperature, and its collective velocity, the proton inclusive cross sections are determined. The resulting predictions of the model fit the gross features of the proton inclusion spectra surprisingly well. For the case of $^{20}\text{Ne} + \text{U}$ at 400 MeV/ n , a characteristic fireball with ~ 60 nucleons, 50 MeV in kT , and a collective velocity of $0.27c$ adequately described the data.

Besides the macroscopic fireball model, microscopic calculations of the proton inclusive spectra have also been developed using several other approaches but have, to date, not been any more successful in accounting for the data. These approaches include a wide variety of models: intranuclear cascade models,^{15–17} fluid dynamical models,¹⁸ calculations using hard-sphere scattering,¹⁹ and classical many body equations of motion procedures.^{20,21}

With regards to the composite particle spectra, no microscopic calculations have as yet been attempted. However, the inclusive spectra of these composite particles have been interpreted in terms of a phenomenological model in which nucleons with small relative momentum coalesce.⁷ This imposed momentum space restriction leads to correlations in energy and angle between double differential cross sections for composite particles and powers of the corresponding proton cross sections. This correspondence is borne out by the experimentally determined cross sections as shown in Ref. 7. Now, in Ref. 10 an alternate model was proposed which also accounts for the correlation between composite particle and proton cross sections. It is the development of this latter model that is now to be discussed.

B. Explosive nucleosynthesis and equilibrium thermodynamics

Here, a qualitative discussion for the foundations of the model is presented. The underlying

picture for the formation of composite nuclei to be developed is one of an expanding collection of strongly interacting nucleons raised to a high temperature which evolves from a high density region to a low density free expansion. Now, in the initial stages of the expansion, when densities are high and mean free paths are small compared to the size of the system, collisions are then frequent, causing scattering to all possible states. These collisions will then have a threefold role. First, they will produce the thermal equilibrium generating the randomized final state from the ordered initial state.^{22,23} Secondly, they will lead to particle production ($N+N \rightarrow N+N+\pi$) and transformation ($N+\pi \rightarrow \Delta$) when incident incoming energies are above particle production thresholds.⁴ Thirdly these interactions result in composite particle formation and breakup ($n+p \rightleftharpoons d$).

Then, in the initial stages, when interactions are important, transformations and transitions occur between all strongly interacting constituents so that a transient character is ascribed to each element of the system. Only conserved quantities will have a permanence. For example, a "deuteron" (or more precisely, a pair correlation) will be a *metastable resonance* in the interacting stage which will appear at one point and then disappear only to reappear at another point possibly in a disguised form with a Δ replacing a nucleon.

Now, the high temperatures ($kT \sim 50$ MeV) and densities ($\rho \sim$ nuclear matter) involved in the interaction region also imply that composite particles can be produced in a profusion of reactions whose rates will be large since energies encountered ($\langle E \rangle \sim \frac{3}{2}kT \sim 75$ MeV) are above all barriers. Furthermore, if these rates are comparable or shorter than expansion time scales, then the rates of formation for various reactions become equal to the rates of their breakup (detailed balance) and a chemical equilibrium between all constituents is achieved. Under these circumstances, the dynamical build up of various nuclei quickly takes the system to its equilibrium distributions.²⁴ In turn, properties of phase space distributions, which, for example, maximize the entropy of the distribution of products in this space, play a more fundamental role than the details of the various cross sections.

If a complete thermodynamic equilibrium is established, then the average behavior of the system is describable in terms of a few state functions which will be taken as the volume of the interaction region and the temperature of the system. It is important to note that the establishment of thermodynamic equilibrium in this volume destroys the history of the system for all previous times except for the information related to con-

served quantities. As an example, the number of α particles will reflect a randomized state of the system at some volume and temperature, and will not reflect, except for nucleon number conservation, the ordered initial state. Similarly, any exotic previous state of the system which must evolve through a quasiequilibrium state of the system at some later stage in the time development of the system will also have its information lost, except for any conserved quantities related to it.

In the results to be presented below, the volume of the interaction region (or density of the system) is a physical quantity that will remain in the final expressions; this volume can therefore be extracted. Specifically, the volume reflects an idealization of the dynamic space-time evolution of the system, representing a sharp cutoff from an interacting to a noninteracting system as it expands. *The metastable resonances in this transition eventually become the stable composites.* Thus, in an equilibrium model, the observed properties will reflect a "frozen in" equilibrium distribution of an emitting system as it evolved through space and time. Within the framework to be developed, interactions and their ranges are then both included in producing thermal and chemical equilibrium and in determining the size of the volume where they are established. As it will be shown, this idealization can lead to a complete solution to an otherwise complicated problem of which only a piece (the proton inclusive spectra) has been developed numerically, apart from the macroscopic model of Ref. 6, in rather detailed calculations.

An attempt will now be made to justify an initial thermodynamic equilibrium by first considering the time scales in the expansion of the system, and then by investigating the reaction rates in the dynamical buildup toward equilibrium. However, no attempt will be made to study the actual dynamics of the initial collision of the incident and target nuclei by any detailed microscopic calculation to see if a localized collection of nucleons is generated. Rather, this underlying picture is assumed and consequences and further justifications around this picture are developed.

C. Dynamical considerations

1. Expansion time scales—Hubble model

In order to see if chemical equilibrium can be achieved an estimate of the expansion time scale of a heated system of nucleons is needed. Here, such an estimate is developed in a free expansion model. The model assumes that each point in the distribution of matter is a source of an explosion producing fragments moving radial outward as shown in Fig. 1. Using Hubble's relationship, that

the speed $|\vec{v}|$ outward is proportional to the radial distance R_i from the source point

$$|\vec{v}| = R_i H, \quad (1)$$

a point source velocity distribution $f(\vec{v})$ can be converted into a density distribution: $\rho[\vec{R}_i, t] = H^3 f(|\vec{v}| = R_i H) = t^{-3} f(R_i/t)$; the t , the reciprocal of the "Hubble" constant H , is the time from the explosion. Next, if a local Maxwellian distribution of velocities at each point is assumed, the resulting density distribution is then a Gaussian:

$$\rho[\vec{R}_i, t] = \left(\frac{3}{2\pi}\right)^{3/2} \frac{1}{(V_T t)^3} \exp[-3R_i^2/2(V_T t)^2]. \quad (2)$$

The $V_T = (3kT/m)^{1/2}$ is the thermal velocity obtained by setting the mean energy equal to $3kT/2$, with T being the temperature of the nucleons. The above result can then be used to obtain the density distribution of any initial configuration of matter by performing a simple folded integration over the given initial density distribution. This procedure, when applied to an initial configuration of matter uniformly distributed over a sphere of radius R_s , results in

$$\rho[\vec{R}, t] = \rho_0 \left(\frac{1}{2} \left(\operatorname{erf}\{(R+R_s)[\alpha(t)]^{1/2}\} \mp \operatorname{erf}\{|R-R_s|[\alpha(t)]^{1/2}\} \right) + \frac{1}{2(\pi\alpha(t)R)^{1/2}} \left\{ \exp[-\alpha(t)(R+R_s)^2] - \exp[-\alpha(t)(R-R_s)^2] \right\} \right), \quad (3)$$

with $\alpha(t) = 3/2(V_T t)^2$ and erf an error function; the plus is for $R < R_s$ and the minus for $R > R_s$. The result of Eq. (3) is shown in Fig. 1, from which it can be seen that the characteristic time for the system to go to $\frac{1}{2}$ its original density is, as expected, R_s/V_T . For temperature and sizes of interest, this characteristic time is $\sim 5 \times 10^{-23}$ sec. This result is comparable to the hydrodynamic time R_s/V_s , where V_s is the velocity of sound, which for an ideal gas is

$$\frac{V_s}{c} = \left(\gamma \frac{kT}{mc^2} \right)^{1/2}, \quad (4)$$

with $\gamma = \frac{5}{3}$. Thus, there is little change introduced into the characteristic time when simple refinements, such as compressibility, are incorporated. Also, the expansion time is not a sensitive function of the initial configuration as can easily be seen by evaluating the characteristic time for other reasonable initial configurations. As an example, an initial Gaussian distribution

$$\rho[R, t=0] = \rho_0 \exp[-R^2/R_s^2(0)] \text{ unfolds as}$$

$$\rho[R, t] = \rho_0 \frac{R_s^3(0)}{R_s^3(t)} \exp[-R^2/R_s^2(t)], \quad (5)$$

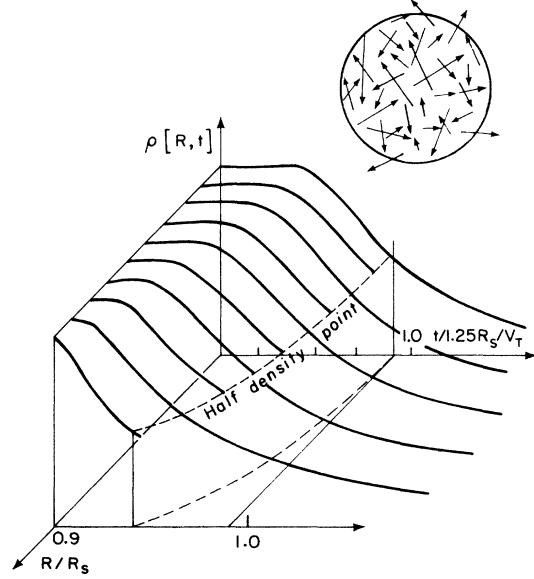


FIG. 1. The free expansion model and its density profile as a function of position and time for points inside the initial uniform sphere.

where $R_s^3(t) = [R_s^2(0) + (\bar{V}_T t)^2]^{3/2}$, with $\bar{V}_T^2 = 2V_T^2/3$. Again the characteristic time scale is R_s/V_T . The expansion time will now be compared to the reaction rate time for nucleosynthesis.

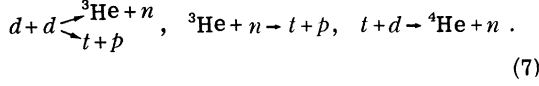
2. Reactions and reaction rate time scales

As already mentioned, the starting point of our description of nucleosynthesis is a dense and heated initial state of protons and neutrons which then combine through a complex set of nuclear reactions to form the various nuclei during the space-time evolution of the system. The mathematical framework for a description of the dynamical formation of nuclei has already been developed in investigation of element formation in the expansion of an isotropic and homogeneous universe^{11,12,13,25} and in imploding-exploding supermassive stars.¹³ By way of illustration and for contrast, let us consider the former case which might have also evolved from an initial dense hot state. The nucleosynthesis proceeds in this situation through a complex set of two body reactions occurring at temperatures $10^9 - 10^{10}$ K, or $kT \sim 0.1 - 1$ MeV, with the first element of the chain being a radiative

capture



After this first electromagnetic interaction, elements are generated by a series of sequential two body nuclear reactions of the type



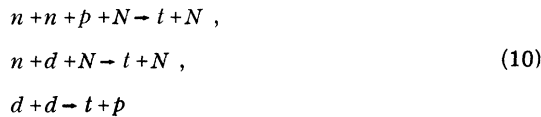
Now it is important to realize that the mechanism of deuteron production is too slow in the relativistic heavy-ion case for the expansion time scales considered in the previous section. Specifically, for temperatures $T \sim 0.5 \times 10^{12}$ K ($kT = 50$ MeV) the inverse reaction can proceed through a giant dipole resonance, whose width is several MeV and whose maximum cross section is ~ 1 mb at an energy ~ 12 MeV, but the resulting reaction rate of $\sim 10^{19}/\text{sec}^{26}$ is still too slow to produce any deuterons during the expansion time scale of $\sim 5 \times 10^{-23}$ sec obtained in the previous section. Thus, the first step must then be a three body reaction



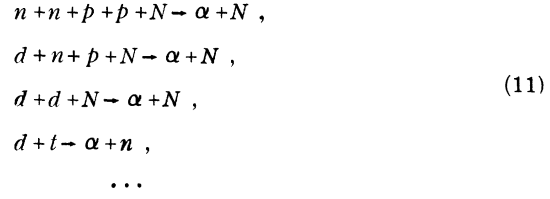
where the nucleon N acts as a catalyzer carrying away the excess energy and momentum to allow the fusion. By comparison, the three body process is not important for deuterium production in an expanding universe where element synthesis occurs when densities are very much lower. In the relativistic heavy-ion case, however, synthesis occurs precisely when densities are near those of nuclear matter so that multinucleon collisions are important. Therefore the dynamical reaction mechanisms for nucleosynthesis are different due to the scale change in the coordinate not being compensated by the scale change in time. In fact, a whole profusion of reactions, besides the sequential two body ones of Eq. (7), are all important with examples as follow:



for deuterons;



for tritons; for ${}^3\text{He}$, change all protons into neutrons and all neutrons into protons in Eq. (10), and for α particles



The dynamical expressions governing the formation of various nuclei for the above reactions can be obtained from a coupled set of first order differential equations which have the same formal structure as those used in Refs. 11 and 13. For example, deuterium formation through the reaction of Eq. (8) is given by

$$\begin{aligned} \frac{d\rho_d}{dt} &= \left[\rho_p \rho_n \left(\frac{\rho_d}{\rho_p \rho_n} \right)_{\text{eq}} - \rho_d \right] \\ &\times \rho_N \langle \sigma(N+d \rightarrow n+p+N) v_{\text{rel}} \rangle , \end{aligned} \quad (12)$$

where ρ_p , ρ_n , ρ_N , and ρ_d are the proton, neutron, nucleon, and deuteron density, respectively. The $(\rho_d/\rho_p \rho_n)_{\text{eq}}$ is the equilibrium ratio of deuterons to protons and neutrons and is a function of temperature only. This ratio, which is derived in Sec. IIIB, is given by the following equation:

$$\left(\frac{\rho_d}{\rho_p \rho_n} \right)_{\text{eq}} = (\lambda_T^3)^{A-1} \frac{A^{3/2}}{2^A} \mathfrak{z}_{\text{int}}(Z, N) \quad (13)$$

with $A = 2$. Here, the λ_T is the thermal de Broglie wavelength given by

$$\lambda_T = \frac{h}{(2\pi m k T)^{1/2}} . \quad (14)$$

The $\mathfrak{z}_{\text{int}}[Z, N]$ is the internal partition function of the composite

$$\mathfrak{z}_{\text{int}}(Z, N) = \left(\sum_j (2s_j + 1) e^{-E_j/kT} \right) e^{|\mathcal{E}_0|/kT} , \quad (15)$$

with the sum in Eq. (15) running over the ground and excited states of the composite and E_j being the energy measured from the ground state energy E_0 . For deuterons $2s_0 + 1 = 3$ and $|E_0| = 2.2$ MeV.

The $\sigma(N+d \rightarrow n+p+N)$ appearing in Eq. (12) is the breakup cross section of deuterium and v_{rel} is the relative velocity of an N, d pair. The product σv_{rel} is to be averaged over the distribution of relative velocities of this pair. When thermal equilibrium has been achieved [which has been assumed in Eq. (12)], the nucleons and deuterons each have a Boltzmann distribution. Noting that the product of two such distributions can again be written as a Boltzmann distribution of relative motion for a particle of reduced mass $\mu = m_1 m_2 / (m_1 + m_2)$ and a Boltzmann distribution for a particle of total mass $M = m_1 + m_2$, the average $\langle \sigma v_{\text{rel}} \rangle$ is easily obtained in the nonrelativistic limit as

$$\langle \sigma v_{\text{rel}} \rangle = \left(\frac{8}{\pi \mu} \right)^{1/2} \left(\frac{1}{kT} \right)^{3/2} \int_0^{\infty} E \sigma(E) e^{-E/kT} dE. \quad (16)$$

A point to note is that $E e^{-E/kT}$ peaks at $E = kT$ and has a mean at $2kT$, so that the breakup cross section contributes over a broad energy range from the threshold energy up to several times kT .

The above simplified illustration can next be generalized to define a dynamical approach to nucleosynthesis in an expanding system which can be summarized as follows. First, write a set of reactions that build nuclei of the type given by Eqs. (9)–(11). Secondly, solve a set of coupled first order differential equations of the form of Eq. (12) in an expanding system with some model for $\rho(t)$ and $T(t)$. Thirdly, when the rates of reactions, governed for instance by $\rho_N \langle \sigma(N+d \rightarrow n+p+N) v_{\text{rel}} \rangle$ for Eq. (8), are large compared with $\dot{\rho}(t)/\rho(t)$ take the instantaneous equilibrium distributions given by Eq. (13) for the densities. The dynamic solution is then the equilibrium thermodynamic solution. In equilibrium $d\rho[Z, N]/dt = 0$ and the rates of production of a given specie become equal to the rates of absorption so that detail balance is achieved. The dependence of $\rho[Z, N]$ on the details of the cross section then vanishes and the concentrations are state functions determined by phase space factors alone. Nevertheless, breakup cross sections will have a hidden role in establishing the equilibration time scale.

Since breakup cross sections have not been measured over the broad energies needed to evaluate Eq. (16) and in many cases have only been determined at a few energies, if at all, it is quite difficult to give an accurate evaluation of the integral in Eq. (16) and to establish the equilibration times. For the case of the deuteron, measurements of $p+d \rightarrow n+p+p$ give 100 mb at 77 MeV and $p+d \rightarrow p+d$ is 50 mb at this energy.²⁷ Measurements have also been reported²⁸ for $d+d \rightarrow n+n+p+p$, $d+d \rightarrow d+n+p$, $d+d \rightarrow p+t$, and $d+d \rightarrow d+d$ for energies 20–50 MeV. The sum of the first two cross sections is 410 mb, the third, 40 mb, and the fourth, 540 mb. There is also one other measurement that we know of for $p+d \rightarrow p+p+n$ at an energy of 14 MeV for which the cross section is 196 mb. A very approximate evaluation of $\langle \sigma v \rangle$ can then be obtained by taking a mean cross section for breakup of 100 mb from which it follows that the product $\rho_N \langle \sigma v \rangle = \lambda \approx 2.5 \times 10^{23}/\text{sec}$ at normal density. The reciprocal of λ determines the time the system takes to reach equilibrium in the deuteron concentration. This time is much shorter than the expansion time of the previous section.

In fact, and fortunately so, a mean breakup cross section (averaged over the distribution of relative energies) of only 10 mb is sufficient to achieve

equilibrium at normal density. Moreover, at relative energies greater than a few times the binding energies of light nuclei, the total fragmentation cross sections of light nuclei should not be very different from the geometrical values πR^2 , which is much larger than 10 mb = 1 fm². Another point to note is that light nuclei have small thresholds for complete fragmentation so that very little of the contribution in the integral of Eq. (16) is lost due to threshold effects. Also, penetration factors, so important in nucleosynthesis in stars, are unimportant here owing to the very high temperatures introduced by the collision. Thus, despite the lack of detailed cross section measurements, there is still good indication that a complete thermodynamic equilibrium can be established.

D. Condition for a quasiequilibrium

Before proceeding to a quantitative discussion of a thermodynamic model it is interesting to develop a condition to determine whether or not a quasiequilibrium is achieved. This can be obtained by first noting that the reaction rates which govern the approach to equilibrium are determined by quantities such as

$$\lambda = \rho_N \langle \sigma(\text{bu}) v_{\text{rel}} \rangle, \quad (17)$$

where $\sigma(\text{bu})$ are breakup cross sections. Now, if λ is greater than $\dot{\rho}/\rho$, then concentrations will have reached their equilibrium values. On the other hand, if λ is less than $\dot{\rho}/\rho$, nuclei will not have been built to their equilibrium concentrations. Letting $t_{1/2}$ be the time it takes the density to drop to $\frac{1}{2}$ its original value, the following equation is obtained

$$\frac{\dot{\rho}}{\rho} = \frac{1/2 \rho}{t_{1/2} \rho} \sim \frac{1}{t_{1/2}} \sim \frac{V_T}{R}. \quad (18)$$

The V_T is the thermal velocity and R the radius of the system. Since ρ varies like R^{-3} , λ will eventually cross $\dot{\rho}/\rho$ if it is initially greater than it because $\dot{\rho}/\rho$ varies with a smaller negative power of R . As an example, an adiabatic expansion of an ideal gas has $R^3 T^{3/2} = K$, so that $V_T \sim 1/R$ and $\dot{\rho}/\rho \sim R^{-2}$. Thus, a primitive condition for a "freeze out" at some equilibrium concentration is

$$\rho_f \langle \sigma_{\text{bu}} v \rangle \frac{R}{V_T} = 1. \quad (19)$$

Defining a nucleon induced mean thermal breakup cross section by $\langle \sigma_{\text{bu}} v \rangle = \bar{\sigma}_{\text{bu}} V_T (8m_N/3\pi\mu_{N,A})^{1/2}$ Eq. (19) can be written as

$$\rho_f = \frac{1}{\bar{\sigma}_{\text{bu}} (m_N/\mu_{N,A})^{1/2} R}, \quad (20)$$

where the inessential $8/3\pi$ is neglected; $\mu_{N,A} = m_A m_N / (m_N + m_A)$. The result of Eq. (20) is just the statement that the mean free path for absorption is equal to the size of the system. It is also interesting to note that Eq. (20) can be developed even further when it is realized that the sum of all inelastic cross sections at high temperatures for a given light nucleus is the total geometrical cross section:

$$\sum_{\text{inelastic channel}} \sigma(N+A) \cong \pi(R_A + R_p)^2. \quad (21)$$

Then, ρ_f is related to the finite size of the composite nucleus for a light nucleus where threshold effects do not play an important role in any of the fragmentation channels and, specifically, in the evaluation of Eq. (16). When these circumstances are met, the following relationship is obtained:

$$\rho_f(A) = \left[\pi(R_A + R_p)^2 R \left(\frac{m_N + m_A}{m_A} \right)^{1/2} \right]^{-1}. \quad (22)$$

Equation (22) implies that in the space-time evolution of the system, a metastable resonance becomes a stable composite nucleus in a transition region when the density of the system is related to the finite size of the composite.

III. PREDICTION OF AN EQUILIBRIUM MODEL—SIMPLEST VERSION

A. Simplified view and its Gibbs grand canonical partition function

Starting with the assumption that the average behavior of a system of nucleons, nuclei, and particles produced in a central collision of two heavy ions at relativistic energies might approximate a thermodynamic system in equilibrium, the hope is that the simple and elegant mathematical framework of equilibrium thermodynamics can lead to some useful insights into the collision. With this qualification in mind, we will proceed on two levels of complexity, the simplest level being defined by a model with the following constraints:

- (1) Impose the condition that the interactions have produced a thermal equilibrium.
- (2) Impose the condition that the interactions produce composite nuclei in their bound states with all species in chemical equilibrium.
- (3) Neglect the structure in the continuum due to the unbound states.
- (4) Otherwise treat particles as noninteracting ideal gases.

Here, particle production will not be considered. The results can easily be extended to include production, but Refs. 4 and 29 already discuss a system of nucleons and pions in equilibrium. Furth-

ermore, the effects of relativity and statistics will also be neglected. Their effects on the composite particle spectrum are small for the densities, temperatures, and energies that are investigated here. In Appendix A, the thermodynamic results including relativity and statistics are summarized for completeness.

Now, the above model leads to a simple and complete solution to the average behavior of a system of nucleons and nuclei in a box of volume V and temperature T . This solution can be obtained from statistical mechanics using the Gibbs grand canonical partition function. For a system of noninteracting ideal gases of different species, this partition function is given by

$$\mathcal{L}(V, T, \{\mu_s\}) = \pi_s \left(\sum_{N_s} e^{\mu_s N_s / kT} \mathfrak{z}_{N_s} \right). \quad (23)$$

where μ_s is the chemical potential of specie S and \mathfrak{z}_{N_s} is the canonical partition function for N_s particles of a particular specie. In turn, the canonical partition function with N_s noninteracting particles is

$$\mathfrak{z}_{N_s} = \frac{\mathfrak{z}_1^{(s)N_s}}{N_s!} \quad (24)$$

with $\mathfrak{z}_1^{(s)}$ the one body partition function given by the product of the internal partition function $\mathfrak{z}_{\text{int}}$ for that specie and the ratio of the volume V of the thermodynamic box to the thermal volume defined in terms of the thermal de Broglie wavelength $\lambda_T(s)$:

$$\mathfrak{z}_1^{(s)} = \frac{V}{\lambda_T^3(s)} \mathfrak{z}_{\text{int}}^{(s)}. \quad (25)$$

The internal partition function $\mathfrak{z}_{\text{int}}^{(s)}$ is given by Eq. (15) and the $\lambda_T^3(s)$ by Eq. (14) with $m \rightarrow M_s$.

The connection of thermodynamics to statistical mechanics can next be introduced through the thermodynamic potential Ω :

$$\Omega = -kT \ln \mathcal{L}(V, T, \{\mu_s\}). \quad (26)$$

All thermodynamic properties then follow from Ω .

B. Law of mass action, Boltzmann distributions

The first quantity of interest is the average number of a particular specie in the thermodynamic volume. This number is obtained from the partial derivative of the thermodynamic potential with respect to the chemical potential:

$$N_s = - \frac{\partial \Omega}{\partial \mu_s} = \mathfrak{z}_{\text{int}}^{(s)} \frac{V}{\lambda_T^3(s)} e^{\mu_s / kT}. \quad (27)$$

When the thermal and chemical interaction conditions are imposed on the system an interesting result is obtained. First, imposing the condition of

chemical equilibrium, which is just the statement

$$\mu_{Z,N} = Z\mu_p + N\mu_n, \quad (28)$$

the law of mass action immediately follows:

$$\frac{N_0[Z,N]}{N_0[1,0]^Z N_0[0,1]^N} = \left(\frac{\lambda_T^3}{V}\right)^{A-1} \frac{A^{3/2} \mathfrak{g}_{int}[Z,N]}{2^A}. \quad (29)$$

The λ_T is the thermal wavelength of the proton. When Eq. (29) is converted to a density distribution, Eq. (13) follows. The above result can also be derived by the Darwin-Fowler method or method of steepest descent; this result is also the nuclear analog of the Saha equation for ionization.

Letting \tilde{Z} and \tilde{N} be the total number of protons and neutrons in the system, including those contained in composite nuclei, the following auxiliary conditions must be satisfied:

$$\sum N_0[Z,N]Z = \tilde{Z}, \quad \sum N_0[Z,N]N = \tilde{N}. \quad (30)$$

A solution to Eqs. (29) and (30) is shown in Fig. 2 for the case $kT = 40$ MeV, $\tilde{Z} = 30$, $\tilde{N} = 30$.

Secondly, imposing the condition of thermal equilibrium, which is just the statement that momentum distributions are Maxwell-Boltzmann, the momentum space density of a composite is

$$\frac{d^3 N_0[Z,N]}{d^3 P_A} = N_0(Z,N) \frac{e^{-E_K/kT}}{(2\pi M_A kT)^{3/2}}. \quad (31)$$

The P_A is the total momentum of the composite and E_K is its total kinetic energy $E_K = P_A^2/2M_A$. The phase space distribution of Eq. (31) can be cast into a Lorentz invariant form when Eq. (31) is multiplied by E , since $d^3 P/E$ is a Lorentz invariant phase space element. The E , here, now includes the rest mass.

The above results show that a thermodynamic model gives rise to an isotropic distribution of fragments. Contrarily, the observed cross sections in the laboratory are forward peaked and, thus, apparently nonthermal in this system. The asymmetry is due to the persistence of the longitudinal momentum of the initial incident state required by overall momentum conservation. In order to avoid a major failure of the model on the most trivial of grounds, one has to allow for non-turbulent collective motion coexistent with local thermal equilibrium.³⁰ Then, in some rest system in which this collective motion has been separated off, distributions will again be isotropic. The results of Eq. (31) apply to this rest system if it exists.

The Lorentz transformation of the distribution of Eq. (31) from this rest system to the laboratory

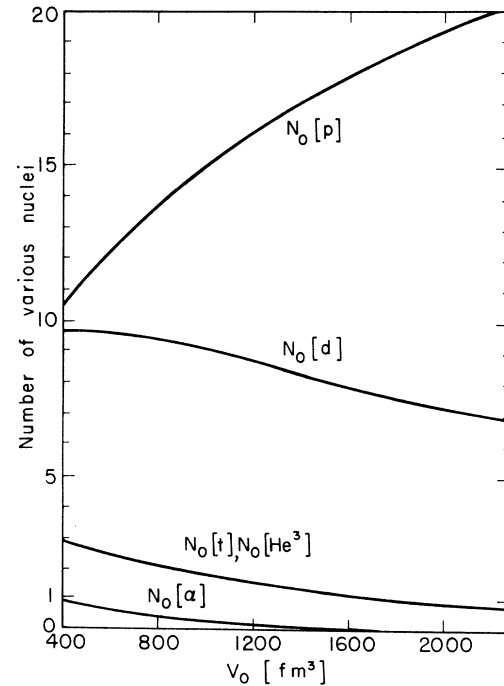


FIG. 2. The number of p , d , t , He^3 and He^4 as a function of the thermodynamic volume. The evaluation is for $kT = 40$ MeV and $Z = 30$, $N = 30$. For 60 nucleons normal nuclear matter occupies a volume of 400 fm^3 . The decrease in the number of nuclei with increasing volume follows from Le Chatelier's principle in thermodynamics. This principle enables qualitative conclusions to be drawn about the direction in which the equilibrium of a system is shifted when changes are made in the external conditions. Specifically, an increase in the volume at constant temperature results in the lowering of the total and partial pressures of the system. From Le Chatelier's principle, the equilibrium of the system will tend to move in such a direction as to oppose this change. This is accomplished by increasing the number of degrees of freedom in the system which will happen when composite structures are broken up into their constituents.

system gives rise to a forward peaking of the distribution. If, for example, this rest system moves with velocity β with respect to the lab, then from the Lorentz invariance of $E d^3 N/d^3 p = E' d^3 N/d^3 p'$, the phase space distributions in the laboratory are

$$\frac{d^3 N_0[Z,N]}{d^3 P_A} = \frac{E'}{E} N_0[Z,N] \frac{e^{-E'_K/kT}}{(2\pi M_A kT)^{3/2}}. \quad (32)$$

The primed quantities refer to the rest system and the unprimed quantities to the lab system. The energy E' can be written in terms of the laboratory energy E through the relationship $E' = \gamma(E - \beta P_A \cos \theta_L)$, where $\gamma = 1/(1 - \beta^2)^{1/2}$ and θ_L is the angle between \vec{P}_A and $\vec{\beta}$. The $E'_K = E_K - \beta P_A \cos \theta_L + \frac{1}{2} M_A \beta^2$ in the nonrelativistic limit.

C. Observed spectrum of nuclei and protons

As shown and discussed in Ref. 6, the proton inclusive cross sections can be accounted for by emission from a thermally equilibrated source (the fireball) moving with a velocity $\beta \sim 0.27$ and having a temperature $kT \sim 50$ MeV for $^{20}\text{Ne} + \text{U}$ at 400 MeV/n. The model fits the data best above 80 MeV/n with some disagreement appearing below this energy. In this lower energy range the proton data can be fitted with a smaller temperature of 40 MeV and a lower velocity of $\beta = 0.15$ or $\beta = 0.175$ as shown in Fig. 3. However, the higher energy parts of the spectra no longer agree with the thermal spectra for the lower temperature and velocity. On the other hand, for the composite nuclei d , ^3He , and ^4He , the higher temperature and velocity fails to fit the inclusive cross sections, but the lower temperature of 40 MeV and lower velocity of 0.15 accounts for the general trends of the cross sections as also seen in Fig. 3.

Inclusive cross section measurements of heavier fragments which include Li, B, C, N, O, and F,

in the energy range 15–60 MeV/n and angular range 35° – 85° for $^{20}\text{Ne} + \text{U}$ at 400 MeV/n and Ar on Au at 500 MeV/n have also been reported.⁸ These cross sections have been fitted with Maxwellians with a temperature of $kT = 52$ MeV with an emitting source moving at $\beta = 0.076$ for $^{20}\text{Ne} + \text{U}$, and with $kT = 65$ MeV and $\beta = 0.085$ for Ar + Au. A similar set of measurements on Li, Be,^{7,9,10} B, C, N, and O at slightly lower energies, in general, than those of Ref. 8, but in a broader angular range can also be accounted for by Maxwellians with temperatures $kT \sim 27$ MeV and $\beta = 0.06$ for $^{20}\text{Ne} + \text{U}$ at 400 MeV/n.⁵

From the above results the following observations are in order. While the proton inclusive cross sections below 100 MeV and the deuteron, triton (not shown), and helium inclusive cross sections are adequately accounted for by a single temperature and velocity for the emitting source, the proton data above 100 MeV and the heavier composite particle data cannot be accounted for by these temperatures and velocities. The discrepancy with the proton data at higher energies and forward

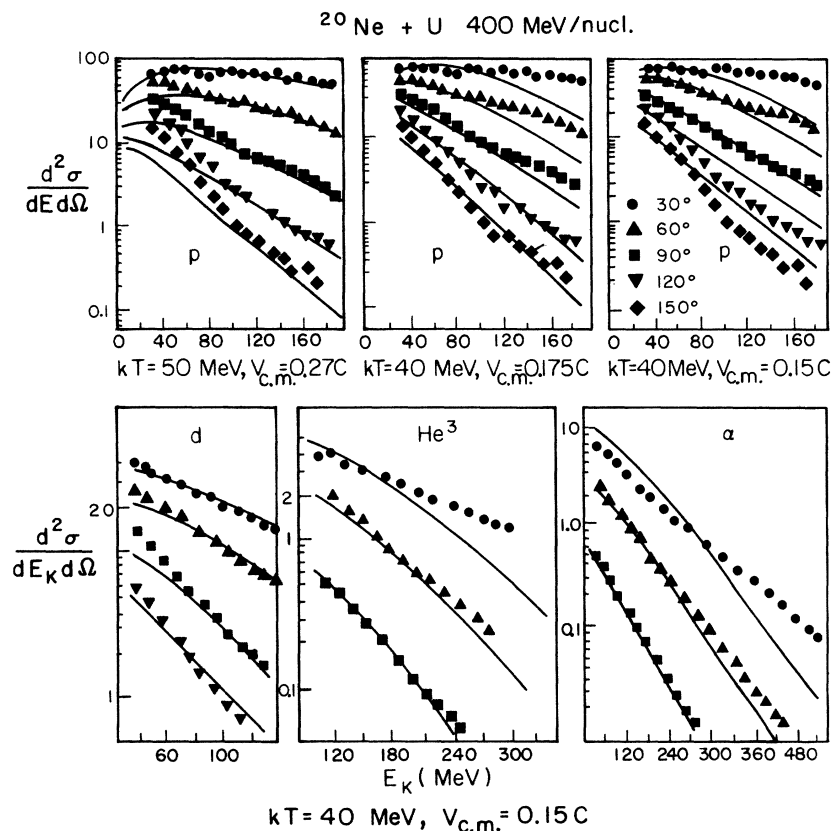


FIG. 3. Double differential cross section fits for protons, deuterons, and helium nuclei. The fit to the proton data for $kT = 50$ MeV and $\beta = 0.27$ is from Ref. 6. The normalization in the predicted deuteron, triton, and α -particle cross sections is left arbitrary since the magnitudes are determined by the thermodynamic volume.

angles may be due to pre-equilibrium processes or may be accounted for by assuming that the spectrum is the product of various sources each with a different temperature and velocity. A third possibility is to assume a different mechanism at different impact parameters.⁵ For the heavier fragments of Li to F, the disagreement between the parameters obtained from the different sets of data is a puzzle. A suggested explanation of the lower temperature and velocity obtained from the data of Ref. 5 is through a complete target explosion in the most central collisions in which the total available inelastic energy is shared among all the nucleons of the target and projectile.⁵ On the other hand, the high temperature and low velocity obtained in Ref. 8 are not apparently explained by this mechanism and a nonthermal source has been proposed.⁸

D. Space-time structure of the emitting region without Hanbury-Brown and Twiss correlation measurements

The space-time evolution of the interacting system of nucleons and nuclei is further investigated here. For this purpose two-particle and multiparticle inclusive experiments are a valuable tool owing to their more exclusive nature. For example, a well known procedure for obtaining the size of an emitting region is due to Hanbury-Brown and Twiss³¹ who obtained the size of a star (α Canis Majoris A) by observing photon-photon correlations with an intensity interferometer. An extension of this technique has also been developed for high energy physics studies^{32,33} and the procedure has recently been used to determine the size of the hadronic region through π - π correlation measurements.³⁴ Similarly, proton-proton correlation measurements have been proposed as a method for studying the space-time history of highly excited nuclei⁴⁹ and exploding nuclei.^{49,50}

All of the above methods are two-particle inclusive methods and rely on determining correlations induced by the Bose-Einstein or Fermi-Dirac nature of these particles. Here, we propose a simpler method which utilizes an advantage of high energy heavy-ion collisions in that a significant fraction of deuterons, tritons, and helium nuclei, along with protons and pions, is observed.

The essential point to note is that an inclusive cross section measurement of a composite particle made up of A nucleons is really an A -particle inclusive measurement of a highly correlated system bound together by the nuclear force in a particular space, spin, and isospin state. As an illustration, an inclusive cross section measurement of a deuteron is a two-particle inclusive measurement of a space symmetric, spin 1, and isospin 0 state of

an n - p system bound together into a stable composite. In the thermodynamic picture discussed in Sec. III B, the history of this detected event can be traced back to the thermodynamic interaction region where it was an n - p correlated metastable resonance which became the stable composite in the dynamic space-time evolution of the system as it passed from the interacting to the noninteracting stage. Thus, deuterium and the other composite nuclei contain, within this framework, idealized snapshots of the space-time history of the emitting region.

To explore this space-time history quantitatively, use is made of Eqs. (29) and (31). By defining the momentum per nucleon $\vec{P}_n = \vec{P}_A/A$, the kinetic energy per nucleon $\epsilon_{\kappa} = E_{\kappa}/A$, and noting that a Boltzmann factor in total energy is the A th power of the Boltzmann factor in energy per nucleon, the following equation can be easily derived¹⁰.

$$\frac{d^3 N_0[Z, N]}{d^3 P_n} = A^3 \mathfrak{Z}_{\text{int}}[Z, N] \left(\frac{h^3}{V} \right)^{A-1} \times \left(\frac{N_0[0, 1]}{N_0[1, 0]} \right)^N \left(\frac{d^3 N_0[1, 0]}{d^3 P_n} \right)^A. \quad (33)$$

From this equation it follows that the A -particle nucleus inclusive spectrum is the A th power of the single-particle proton inclusive spectrum. In turn, this result leads to correlations in energy and angle between double differential cross sections of composite particles and powers of the corresponding proton cross sections.¹⁰ Such correlations in energy and angle have already been observed experimentally⁷ and the results have been interpreted in terms of a coalescence model.⁷ It is therefore worthwhile to briefly state the essential results of this model.

In this latter model, nucleons with relative momentum within a sphere of radius P_0 of each other coalesce and this imposed momentum space restriction leads to the following equation⁷:

$$\left(\frac{d^3 \tilde{N}[Z, N]}{d^3 P_n} \right) = \left(\frac{N_t + N_p}{Z_t + Z_p} \right)^N \frac{(\frac{4}{3} \pi \gamma P_0^3)^{A-1}}{Z! N!} \times \left(\frac{d^3 \tilde{N}[1, 0]}{d^3 P_n} \right)^A. \quad (34)$$

The $d^3 \tilde{N}[Z, N]/d^3 P_n$ is the number of nuclei per event per unit element of phase space. The $\gamma = (1 + P_n^2/m_p^2)^{1/2}$ and the (Z_t, N_t) is the target proton, neutron number and (Z_p, N_p) is the projectile proton, neutron number. Before proceeding any further, it is meaningful to explicitly show two factors in the above relationship which are implicit in P_0 . The first is just a spin alignment factor and consists in multiplying the right hand side of Eq. (34) by $(2s + 1)/2^A$ for the light nuclei which

TABLE I. Values for the coalescence parameters and the thermodynamic region for $^{20}\text{Ne} + \text{U}$ at 400 MeV/n. The ρ_0 is the density of nuclear matter.

Composite	P_0 (MeV/c)	\tilde{P}_0 (MeV/c)	V (fm ³)	ρ_f/ρ_0	\bar{R} (fm)
d	129	71	1340	$\frac{1}{4}$	6.84
t	129	94	842	$\frac{1}{5}$	5.86
^3He	129	94	842	$\frac{1}{5}$	5.86
^4He	142	122	500	$\frac{1}{3}$	4.92

have no excited states. The second factor arises from the fact that the composite particle is at a momentum $\vec{P} = A\vec{P}_n$, so that $d^3\vec{P} = A^3 d^3\vec{P}_n$. This second effect can be incorporated by leaving the left hand side as is and by multiplying the right hand side of Eq. (34) by A^3 . Then, defining a new \tilde{P}_0 by

$$(P_0^3)^{A-1} \equiv A^3 \frac{2S+1}{2A} (\tilde{P}_0^3)^{A-1}, \quad (35)$$

the form of Eq. (34) is unchanged but the trivial spin alignment and phase space position of the composite particle are explicitly removed from P_0 .

Since no explicit reference is made in the coalescence model to the spatial evolution of the cascade nucleons, the interesting relationship of Eq. (34) obtained from it offers no information about the space-time history of the system. On the other hand, an explicit reference is made in an equilibrium model to an interaction volume where thermodynamic equilibrium exists so that expressions derived from it will explicitly contain the volume as shown in Eq. (33). Now, the formal correspondence between Eq. (33) and Eqs. (34) and (35) can be exploited to obtain the values of V from the values of P_0 of Ref. 7. In Table I a summary of the results is given. The table also contains the results for the freeze out density.¹⁰

The information about the size of the emitting system contained in the composite particle inclusive cross sections refers only to the total volume and not to its linear dimensions. In order to obtain information about the longitudinal and transverse dimensions, a more detailed Hanbury-Brown-Twiss two-particle inclusive experiment has to be done which explores the two-particle phase space distribution away from the single line representing the deuteron. However, a mean linear dimension can be defined by

$$\frac{4}{3}\pi\bar{R}^3 = V \quad (36)$$

and the composite particle data can be used to obtain a linear dimension for the size of the emitting region. Only in a conspiracy of a very elongated

ellipse will the extracted \bar{R} be far from the true linear dimensions in the longitudinal and transverse directions. With this reservation noted, the mean linear dimensions are given in Table I.

The results quoted in this table show that the size of the emitting region varies from ~ 5 to ~ 7 fm depending on the nucleus. While this might at first be thought of as an undesirable feature in a thermodynamic model, since it would be best to have a single set of equilibrium conditions to explain all the data, it does show that α particles may be emitted at an earlier stage in the evolution than t and ^3He , which are then followed by deuterons. In fact, the results of Sec. II D suggest precisely this behavior owing to the finite size of the composite particles. Moreover, objections to a thermodynamic approach which gives different volumes when dealing with point particles, may not apply to a thermodynamic description of a collection of composite structures with finite sizes.

Finally, it should be emphasized that Planck's constant h appears in the phase space distribution of Eq. (33) and in the chemical equilibrium expression of Eq. (29). Thus, unlike the coalescence model result of Eq. (34), the solution developed here for the phase space distribution of composite particles has a quasiclassical nature. The origin of Planck's constant in the above expressions arises from the fact that in a chemical transformation the number of degrees of freedom is changed; in turn, this change leads to a dependence of the thermodynamic properties of the system on the fundamental volume in phase space from which the number of dynamical states making up the thermodynamic state is to be calculated. Alternately, the first and second laws of classical thermodynamics leave the law of mass action of Eq. (29) unspecified owing to the appearance of undetermined entropy constants resulting from the lack of a well defined unit of action in classical descriptions. Only by introducing the nonclassical third law of thermodynamics or Nernst's theorem is this ambiguity removed from classical thermodynamics. But imposing the constraint of the third law must also introduce Planck's constant into the description of the phase space distribution of products.

E. Comparison with the Butler-Pearson model
for deuteron formation

This subsection is devoted to a brief discussion of the Butler-Pearson model³⁵ for deuteron production in high energy proton collisions with nuclei. The two step formation mechanism proposed in their model involves: (i) the two body interaction between pairs of cascade protons and neutrons and, (ii) the collective mean field of the rest of the nucleus which acts as the third body necessary for energy and/or momentum conservation. Using second order time dependent perturbation theory, Butler and Pearson developed the following approximate expression for the probability of formation of deuterons with wave number \vec{K} [Eq. (21) of Ref. 35]:

$$n(\vec{K}) = 2 \left(\frac{48\pi C m}{\hbar} \right)^2 \left(\frac{V_0}{K} \right)^2 I(R_0) [P(\frac{1}{2}\vec{K})]^2. \quad (37)$$

$$I(R_0, \gamma) = \int_0^\infty \eta d\eta [G(\eta)]^2 \int_0^\infty \zeta^2 d\zeta \left[\frac{4}{(\zeta^2 + a^2)^2} + \frac{2}{(\zeta^2 + \frac{1}{4}\eta^2 + a^2)^2 - \zeta^2 \eta^2} - \frac{1}{\eta \zeta} \left(\frac{4}{(\zeta^2 + a^2)} - \frac{1}{(\zeta^2 + \frac{1}{4}\eta^2 + a^2)} \right) \ln \left| \frac{a^2 + (\zeta + \frac{1}{2}\eta)^2}{a^2 + (\zeta - \frac{1}{2}\eta)^2} \right| \right]. \quad (38)$$

Here, the $G(\eta)$ is the Fourier transform of the optical potential with η the momentum transfer times R_0 : $\eta \approx K \theta R_0$. The $a = \gamma R_0$ and $\zeta = k_t R_0$, with k_t the internal relative wave number of the two nucleons that eventually comprise the deuteron. In Ref. 35, the above integral is done numerically. Here, it is to be noted that the ζ integral can be done analytically:

$$I(R_0) = I(R_0, \gamma) \equiv \int_0^\infty \eta d\eta [G(\eta)]^2 I(\eta, \gamma R_0 = a), \quad (39)$$

with

$$I(\eta, \gamma R_0 = a) = \frac{3\pi}{2a} - \frac{8\pi}{\eta} \tan^{-1} \frac{\eta}{4a} + \frac{\pi}{\eta} \tan^{-1} \frac{\eta}{2a}. \quad (40)$$

For $\eta \ll 2a$,

$$I(\eta, \gamma R_0 = a) \rightarrow \frac{3\pi}{5 \times 2^7} \frac{\eta^4}{\gamma^3 R_0^5}. \quad (41)$$

The limit $\eta \ll 2a$ is not so unreasonable since $q = k\theta$ is $\sim R_0^{-1} \sim 0.15 \text{ fm}^{-1}$ for a heavy nucleus, while $2a/R_0 \sim 2\gamma \sim 0.46 \text{ fm}^{-1}$ for the deuteron. Therefore, this $I(\eta, \gamma R_0)$ limit, while not giving the exact dependence of $n(\vec{K})$ on γ and R_0 , will give its qualitative characteristic dependence. From the above results, the dependence of $n(\vec{K})$ on $E_0 \sim \gamma^2$ is $1/E_0^2$ and this behavior has its basic origin in the energy denominator of the second order perturbation development. The decrease of $n(\vec{K})$ with increasing

This probability, the $n(\vec{K})$ of the above equation, is thus related to the square of the cascade nucleon distribution, the $P(\frac{1}{2}\vec{K})$, at one-half the deuteron momentum. The model therefore predicts a power law form of the coalescence⁷ and thermodynamic models.¹⁰ In fact, the coalescence model is just a generalization of a simplified version of the Butler-Pearson model originally due to Schwarzschild and Zupancić³⁶ in which the coefficient in front of $[P(\frac{1}{2}\vec{K})]^2$ is essentially replaced by $\frac{4}{3}\pi P_0^3$. It is now useful to pursue this coefficient further.

First, $C^2 = \gamma/2\pi$, where γ is determined by the deuteron binding energy $E_0 = \hbar^2 \gamma^2 / m$. The V_0 and R_0 appearing in Eq. (37) are the depth V_0 and radius R_0 of the optical potential. Secondly, the $I(R_0) = I(R_0, \gamma)$ is a rather complicated two dimensional integral [Eq. (22) of Ref. 35]:

E_0 is understandable in a final state interaction model since the greater the binding energy of the deuteron, the further away are the initial cascade nucleons from energy and momentum conservation with the final deuteron state and the less likely is the formation probability. With regards to the R_0 dependence of Eqs. (37) and (41), an increase in R_0 results in a reduction of the momentum transfer from the mean field, since $qR_0 \sim 1$, and, in turn, a reduction in the formation probability.

By contrast, an equilibrium approach gives an opposite dependence on binding energy due to an increase in the internal partition function with increasing binding energy. However, the dependence on the traditional Boltzmann factor in binding energy is greatly reduced by the high temperatures involved. On the other hand, the qualitative volume dependence of both models is the same but for different reasons. In a thermodynamic model, the density of states increases with increasing V , so that the entropy of the system will increase when composite structures are converted into their constituents when the volume of the thermodynamic region is increased. In a final state interaction model, the momentum transfer necessary for the coalescence decreases with increasing volume.

Finally, the Butler-Pearson model seems appropriate for proton collisions which produce only a small perturbation on the target system so that an optical potential or mean field is still a meaningful concept. In high energy heavy-ion collisions,

which produce explosive events, the target is not so simply perturbed and the exclusion principle, so important in establishing a mean field, no longer plays such a fundamental role in the dynamics of the collision between nucleons. Therefore, in explosive central collisions a completely different framework for the description of such events is necessary.

F. Other thermodynamic variables: Law of partial pressures, entropy, and equipartition of energy

Some of the other thermodynamic quantities of interest are the pressure P , entropy S , and energy E which are now considered. The equation of state follows from

$$P = - \left(\frac{\partial \Omega}{\partial V} \right)_{T, \{\mu_s\}} = kT \frac{\partial}{\partial V} \ln \mathcal{L}, \quad (42)$$

where Ω is the thermodynamic potential and \mathcal{L} the Gibbs canonical partition function of Sec. III A. Performing the above operation, the law of partial pressures follows:

$$PV = \sum_s N_s kT. \quad (43)$$

Similarly the entropy follows from $S = -(\partial \Omega / \partial T)_{V, \{\mu_s\}}$:

$$S = \sum_s k N_s \ln \frac{e g_{\text{int}}(s) V}{N_s \lambda_T^3(s)} + \frac{3}{2} N_s k. \quad (44)$$

The $g_{\text{int}}(s)$ is the spin degeneracy factor for specie S . Equation (44) is just the Sackur-Tetrode law for a system composed of different species. The constraint imposed by Eq. (28), which leads to connections between the different species through the law of mass action, is such as to make the entropy a maximum since the equilibrium thermodynamic state is just the state of maximum entropy. In fact, Eq. (29) can be derived from S given by Eq. (44), by requiring S to be a maximum.

The total mean energy E can be obtained from a Legendre transformation $E = \Omega + ST + \sum \mu_s N_s$:

$$E = \sum_s \frac{3}{2} N_s kT = \frac{3}{2} PV. \quad (45)$$

The result of this equation is just the statement of equipartition of energy, with each degree of freedom having mean energy equal to $kT/2$.

The expressions of Eqs. (43)–(45) show that the system formally looks like ideal gas of noninteracting particles. However, interactions are included in these expressions as shall now be shown.

G. Equation of state and the virial expansion

The equation of state of Eq. (43) is just the ideal gas result for each specie. Since the actual gas is

nonideal, the equation of state should obey the virial expansion

$$P = \frac{\tilde{A} kT}{V} \left[1 + \frac{\tilde{A}}{V} B(T) + \left(\frac{\tilde{A}}{V} \right)^2 C(T) \right], \quad (46)$$

where $B(T)$, $C(T)$, ... are the second, third, ... virial coefficients. The $\tilde{A} = \tilde{Z} + \tilde{N}$ is the total nucleon number of the system. It might seem at first thought that a contradiction has arisen since each specie contributes as an ideal gas, but the gas is nonideal. However, the resolution of this apparent paradox is quite simple once it is realized that collisions are responsible for the formation of composite structures and for the departures from an ideal gas law. In fact, the chemical equilibrium imposes certain restrictions on the number of different species so that the theory of chemical equilibrium is ultimately related to the virial expansion.

As an illustration of this result, consider a gas of neutrons, protons, and metastable n - p pair correlations—“deuterons.” Letting $N_p = N_0[1, 0]$, $N_n = N_0[0, 1]$, and $N_d = N_0[1, 1]$, and specializing to the situation $N_p = N_n$, the law of partial pressures can be written as

$$P = \frac{N_p}{V} kT + \frac{N_n}{V} kT + \frac{N_d}{V} kT = \frac{\tilde{A}}{V} kT \left(1 - \frac{N_d}{\tilde{A}} \right), \quad (47)$$

where $\tilde{A} = N_p + N_n + 2N_d$. Comparing this result with that of the virial expression, the second virial coefficient can be seen to be

$$B(T) = - \frac{N_d}{\tilde{A}^2} V. \quad (48)$$

The ratio $(N_d / \tilde{A}^2) V$ is obtained from the law of mass action:

$$\frac{N_d}{(\frac{1}{2}\tilde{A} - N_d)^2} V = \frac{2^{3/2}}{4} \lambda_T^3 \mathfrak{g}_{\text{int}}(d). \quad (49)$$

The above results are easily generalized to the higher coefficients in the virial expansion, with $C(T)$ being due to triple correlations plus binary correlations between pairs plus nucleons, etc. In fact, in the simplest version of the model being discussed in this section, the third and fourth virial coefficients are

$$C(T) = -2 \frac{N^3_{\text{He}} + N_t}{\tilde{A}^3} V^2, \quad (50)$$

$$D(T) = -3 \frac{N_d}{\tilde{A}^4} V^3.$$

The numbers of α , ${}^3\text{He}$, t , and d 's are obtainable from the law of mass action, Eq. (29), coupled with the constraint condition of Eq. (30). The results of such an evaluation have already been illustrated in Fig. 2.

It is also a useful exercise to rewrite the equation of state as

$$PV = \bar{A}kT \left(1 - \frac{N_d}{\bar{A}} - 2 \frac{N_{^3\text{He}} + N_t}{\bar{A}} - 3 \frac{N_a}{\bar{A}} \dots \right). \quad (51)$$

An evaluation of the number of d , t , ^3He , and ^4He nuclei results in an approximate 30–40% reduction in the pressure, for densities in the vicinity of one-third nuclear matter, due to the attractive correlations responsible for the bound states.

From the equation of state, the energy density immediately follows using

$$\epsilon(\rho) = \frac{E}{V} = \frac{3}{2}P. \quad (52)$$

The estimate used to obtain the reduction in pressure due to the attractive correlations, can also be used to obtain the increase in temperature for a fixed excitation energy in the system. Namely, the reduction in the degrees of freedom due to the attractive correlations raises the temperature by 30–40%.

Finally from the energy-temperature relationship, the specific heat can be calculated. The importance of the specific heat, $C_v \equiv (\partial E / \partial T)_v$, is that it relates to the change in the slopes of the inclusive spectra resulting from a change in the incident energy of the beam. Now, at reasonably high temperatures, the temperature dependences of the Boltzmann factors in the internal partition functions are not as important as the temperature dependences of the thermal de Broglie wavelengths. This observation then leads to the following equation for the specific heat:

$$C_v = \frac{3}{2}\bar{A}k \left[1 - \frac{1}{2}\rho B(T) - 2\rho^2 C(T) - \frac{7}{2}\rho^3 D(T) \dots \right], \quad (53)$$

where $\rho = \bar{A}/V$. Since the nuclear force is basically attractive in the energy range considered here, $C_v \geq 3\bar{A}k/2$ and $\Delta E/C_v T = \Delta T/T \leq (\Delta T)_{\text{ideal}}/T$. The change in temperature of the system is less than that of an ideal gas, with the difference going into breaking the attractive correlations below particle production thresholds. Above these thresholds, energy goes into making new degrees of freedom. In fact, the temperature may be limited if the number of degrees of freedom increases exponentially.³⁰

IV. NUCLEAR RESONANCES, CONTINUUM CORRELATIONS, AND THE THERMODYNAMIC PROPERTIES OF THE SYSTEM

A. Resonance and echoes

In Sec. III of this investigation, a simplified model was developed in which the structure in the con-

tinuum due to the unbound nuclear states was neglected. Now an attempt will be made to incorporate into the thermodynamic description the scatterings of nucleons and nuclei which produce this structure. The technique to be employed has been developed by Beth and Uhlenbeck³⁷ in their discussion of the second virial coefficient and has since been used by Belenky³⁸ and Hagedorn³⁰ in particle physics in an effort to include the strong interactions which produce the particle resonances into the Fermi statistical model.³⁹

To incorporate this refinement into the thermodynamic model the effect of such collisions on the continuum level density must be evaluated. For binary collisions, the change in level density due to the structure in the continuum can be related to changes in the phase shift due to the interaction. Specifically, the wave function of a pair is asymptotically changed by their mutual interaction to $\sin[kr - l\pi + \delta_l(k)]$. Imposing the boundary condition that the wave function vanish at $r=R$, leads to the condition

$$kR - l\pi + \delta_l(k) = n_l\pi. \quad (54)$$

The number of states per unit k is then changed through the binary interaction by

$$\Delta \frac{dn_l}{dk} = \frac{1}{\pi} \frac{d\delta_l(k)}{dk}. \quad (55)$$

If the interaction produces a narrow resonance compared with kT in a particular l (or J) state, then the internal partition function of the pair acquires a contribution

$$(2J_r + 1)e^{-E_r/kT}, \quad (56)$$

where E_r is the energy and J_r the angular momentum of the resonance. Repulsive components of the force also affect the level density and internal partition function. For example, for a hard sphere gas $\tan\delta_l = j_l(ka_0)/n_l(ka_0)$, where a_0 is the hard sphere radius, and

$$\frac{d\delta_l}{dk} = \frac{-1}{k^2 a_0 [j_l^2(ka_0) + n_l^2(ka_0)]}. \quad (57)$$

Thus, both attractive and repulsive components influence the level density. An attractive resonance produces a unit change in $\Delta dn_l/dk$ across a resonance for which the phase shift changes by π , and thus corresponds to an additional state. On the other hand, an echo of a resonance,⁴⁰ for which the phase shift decreases by π , results in a negative unit change in $\Delta dn_l/dk$ corresponding to the loss of a state. From Levinson's theorem,⁴¹ $\delta_l(0) - \delta_l(\infty) = N_l\pi$, where N_l is the number of bound states; then $\int \Delta dn_l/dk dk$ changes by $-N_l$ over the whole continuum, so that echoes of resonances cancel the resonances and bound states in the level

density. Of course the continuum internal partition function is weighted by the Boltzmann factor:

$$Z_{\text{int}} = \sum_{J,T} \frac{(2J+1)(2T+1)}{\pi} \int \frac{d\delta_{J,T}}{dE} e^{-E/kT} dE \quad (58)$$

and a complete cancellation does not occur owing to the differences in location in the continuum of the echoes and resonances and to the fact that echoes cannot be very narrow since the rate of descent of the phase shift is subject to Wigner's limit⁴² $d\delta_l/dk \geq -R$.

Before proceeding to an evaluation of the effect of resonances in equilibrium thermodynamics it is worthwhile here to mention that resonances also affect a dynamical nonequilibrium model for composite particle formation. Specifically, they act as stepping stones for the formation of nuclei, with a well known example being the formation of ^{12}C in red giant stars through the triple α process which proceeds via an ^8Be resonance to an excited level in ^{12}C .⁴³

B. Correction to the nuclear gas of nucleons

Once the behavior of the phase shifts is known, the results of the previous section allow an evaluation of the partition function. The most thoroughly investigated situation is that of the nucleon-nu-

cleon interaction where a detailed phase shift analysis has been done. Figure 4 illustrates the dependence of these phase shifts on energy.⁴⁴ The results of Eq. (58) then allow an evaluation of the contribution of the continuum interaction to the internal partition function. In Table II, a summary of the results of an evaluation of Eq. (58) is given for the case $kT = 40$ MeV.

The following conclusions can be drawn from the results of Table II. First, the $l=0, S=0, T=1$ interaction contributes $\frac{1}{15}$ as much to Z_{int} as the $l=0, S=0, T=0$ bound state whose internal partition function is $\sim 2S+1=3$. The large reduction of the virtual state is accounted for by the spin degeneracy factor and by the empirical result that the phase shift only goes to 60° and then declines. Secondly, the sum of the p -state contributions in the $T=1$ state is small because of the Serber nature of the force. Thirdly, the $T=0$ phase shift contribution is dominated by the decline of the $l=0, S=1$ phase shift—the “echo” of the deuteron bound state. The results of the above evaluation also allow an estimate of the number of proton-proton attractive pair correlations to the number of neutron-proton attractive pair correlations:

$$\frac{N_{pp}(^1S_0)}{N_{pn}(^3S_1)} \approx \frac{1}{9}. \quad (59)$$

Thus, the attractive component of the nucleon-nucleon interaction predominately makes n - p pair correlations rather than p - p pair correlations.

C. Corrections to the nuclear gas of nucleons plus nuclei

The effect of the excited unbound states of the heavier composites ($l, ^3\text{He}, ^4\text{He}, ^5\text{He}, ^5\text{Li}, \dots$) can also be included by use again of Eq. (58). The resonant states of these nuclei have natural lifetimes that are, in many cases, $\sim 10^{-21}$ sec. This natural lifetime is long compared to the lifetime of the emitting thermodynamic region $\sim 5 \times 10^{-23}$ sec. Therefore, these excited nuclei will leave the equilibrium region intact and naturally decay afterwards, mostly by particle emission, into light nuclei. This natural decay then leads to final

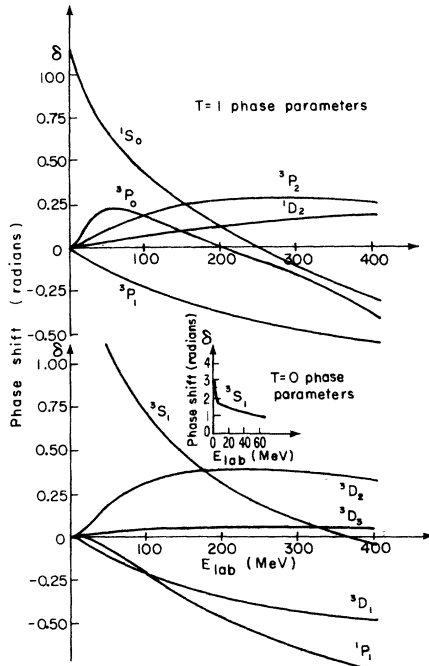


FIG. 4. Nucleon-nucleon phase shift parameters as a function of energy from Ref. 44.

TABLE II. Contributions to the internal partition function.

T=1		T=0	
Phase shift	Z_{int}	Phase shift	Z_{int}
1S_0	+0.2	3S_1	-1.66
3P_0	+0.4	1P_1	-0.12
3P_1	-0.12	3D_1	-0.15
3P_2	+0.14	3D_2	+0.23
1D_2	+0.05	3D_3	+0.05

rearrangements in the spectrum of emitted fragments long after the strong interactions have ceased between the different components of the system.

Before proceeding with a more quantitative discussion, one note of precaution should be stated. This concern arises from the results of Sec. IID and the remarks made in the last paragraph of Sec. IIID. Since the composite nuclei are finite size structures interacting in a region of space whose dimension is increasing due to the expansion, the point at which the system stops interacting for a particular correlated configuration of nucleons is related to the finite dimensions of this structure; these remarks are quantitatively expressed in the relationship of Eq. (22). Now, for a loosely correlated structure, the system will be interacting even at a late stage of the expansion when the density is low so that its concentration is greatly reduced and the possibility of it being

TABLE III. Levels and their contribution to the internal partition function. Level (4) of ${}^5\text{He}$ is included on the basis of charge symmetry even though there is no clear indication for it. The deuteron results are obtained from Sec. IV C.

Nucleus	Level	Exc. energy	Spin	Decay modes	Z_{int}
d	1	0(-2.2)	1^+	$g.s.$	3.15
	2	~2.2	0^+	p, n	0.2
t		0(-8.48)	$\frac{1}{2}^-$	$g.s.$	2.47
${}^3\text{He}$		0(-7.72)	$\frac{1}{2}^-$	$g.s.$	2.43
${}^4\text{He}$	1	0(-28)	0^+	$g.s.$	2.01
	2	20.1	0^+	p	1.22
	3	21.1	0^-	p, n	1.19
	4	22.1	2^-		5.81
	5	25.5	0^+	d, p, n	1.05
	6	26.4	2^-	p, n	5.25
	7	27.4	1^-	p, n, γ	3.16
	8	29.5	0^+	p, n, γ	0.95
	9	30.5	(?0)	p, n, d	0.90
	10	31.0	1^-	p, n, d	2.78
${}^5\text{He}$	1	0(+0.89)	$\frac{3}{2}^-$	n, α	3.91
	2	4	$\frac{1}{2}^-$	n, α	1.81
	3	16.76	$\frac{3}{2}^+$	γ, n, d, t, α	2.62
	(4)	18	$\frac{1}{2}^+$		1.24
	5	19.2	$\frac{3}{2}^+$	n, d, t, α	2.36
${}^5\text{Li}$	1	0(+1.87)	$\frac{3}{2}^-$	p, α	3.80
	2	4	$\frac{1}{2}^-$	p, α	1.72
	3	16.66	$\frac{3}{2}^+$	$\gamma, p, d, {}^3\text{He}, \alpha$	2.55
	4	18	$\frac{1}{2}^+$	$\gamma, p, d, {}^3\text{He}, \alpha$	1.21
	5	20	$\frac{3}{2}^+$	$p, d, {}^3\text{He}, \alpha$	2.31

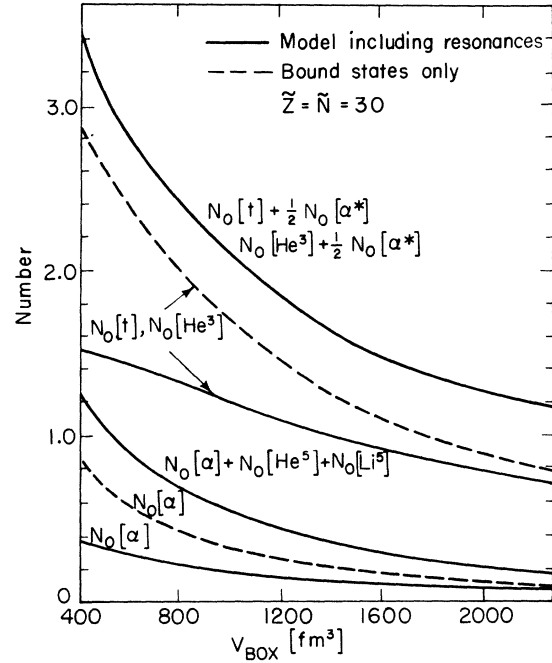


FIG. 5. The number of various species in the thermodynamic volume as a function of this volume. The evaluation is for $kT_0 = 40$ MeV and $Z = 30$, $N = 30$. The solid line includes the resonances listed in Table III, while the dotted line is an evaluation including only bound states.

in thermal equilibrium might also be questioned. Such structures might then best be left out of the state sums or partition function.⁴⁵

To proceed on a more quantitative basis, an evaluation of Eq. (58) is necessary. Since detailed phase shift analyses are not available for the scattering of nucleons and light nuclei off other light nuclei, only a somewhat approximate procedure can be developed. Moreover, the contribution of resonant states is subject to the reservations of the last paragraph. Nevertheless, it is of some interest to see what effect the continuum has within some approximate scheme. Here, the procedure taken is to include the observed low lying resonances that have been reported in Refs. 46-48. Table III lists these observed levels and the internal partition function for each level assuming that each resonance came from a phase shift which changed by π . A temperature of $kT = 40$ MeV was used.

The results of Eqs. (29) and (30) can then be used to arrive at the new distributions of nuclear species in the gas. Figure 5 illustrates the results of the evaluation with these resonances included; also shown are the results of the simplified model of Sec. III which does not include the contribution of any of these resonances. The following features of the figure should be noted. The

number of "bound" α particles, tritons, and ${}^3\text{He}$ is reduced from the simplified model; but, after natural decay of the excited states, the final number of t , ${}^3\text{He}$, and ${}^4\text{He}$ somewhat exceeds the results of the simplified model. However, the two results are within $\sim 20\%$ of each other.

In a model with resonances included, the momentum space density of a nuclear composite has contributions from its bound states and from the decay of resonant states of heavier nuclei. As a concrete example, the momentum space density of α particles has its primary bound state contribution given by

$$\frac{d^3 N_{0\lambda}({}^4\text{He})}{d^3 P_n} = \frac{N_0({}^4\text{He}) A_4^{3/2} e^{-A_4 \epsilon_n / kT}}{(2\pi m_p kT)^{3/2}}. \quad (60)$$

and its secondary contribution from resonant states λ in ${}^5\text{He}$ and ${}^5\text{Li}$ given by (neglecting small recoil corrections)

$$\begin{aligned} \frac{d^3 N_{0\lambda}({}^4\text{He})}{d^3 P_n} &= \sum_{\lambda} \frac{\Gamma_{\lambda}({}^4\text{He}, n)}{\Gamma_{\lambda, T}} \frac{d^3 N_{0\lambda}({}^5\text{He})}{d^3 P_n} \\ &+ \sum_{\lambda} \frac{\Gamma_{\lambda}({}^4\text{He}, p)}{\Gamma_{\lambda, T}} \frac{d^3 N_{0\lambda}({}^5\text{Li})}{d^3 P_n}. \end{aligned} \quad (61)$$

The

$$\frac{d^3 N_{0\lambda}({}^5\text{He})}{d^3 P_n} = \frac{N_{0\lambda}({}^5\text{He}) A_5^{3/2} e^{-A_5 \epsilon_n / kT}}{(2\pi m_p kT)^{3/2}}, \quad (62)$$

with a similar result for ${}^5\text{Li}$. The $A_n = n$ and the $\Gamma_{\lambda}({}^4\text{He}, n) / \Gamma_{\lambda, T}$ is the branching ratio for the state λ to decay into ${}^4\text{He} + n$. The $N_{0\lambda}[Z, N]$ are determined by a procedure already described in the text.

The momentum space density of α particles will be the sum of Eqs. (60) and (61). The following feature of the latter contribution is worth noting. Since equipartition of energy is assumed to hold, each excitation of the system has $3kT/2$ mean energy. Heavier nuclei then have mean speeds that are slower than the lighter ones they naturally decay into so that the resonant state contribution affects the lower energy region of the inclusive spectrum.

A generalization of the results of Eqs. (60) and (61) to all possible resonant deexcitations implies a multicomponent structure to the spectrum arising from the difference in the exponential Boltzmann behavior of the primary and secondary components. Noting that the exponential behavior of the secondary part can be rewritten as $A_s \epsilon_n / kT = A_p \epsilon_n / kT^*$, with $T^* = A_s T / A_p$, it then follows that the slope in a log plot of the momentum space density is steeper for the secondary contribution than for the primary. The A_p is the nucleon number of the primary nucleus and A_s the corresponding number for the secondary. Moreover, since the

secondary contribution affects the lower energy part of the spectrum, the curvature of the spectrum in log plots would be upward from such effects.

Because of the approximate nature of the evaluations presented and the reservations already mentioned about including resonances of loosely bound structures in a thermodynamic description, the results of this section are only meant to be schematic.

V. SUMMARY AND CONCLUSIONS

This investigation concerned itself with the question of the formation of composite particles seen in relativistic heavy-ion collisions. The description developed is analogous to that used in describing the formation of nuclei in the expansion of an isotropic and homogeneous universe and in exploding supermassive stars. The model proposed is then one in which composite structures are formed through a complex set of reactions in the space-time evolution of a rapidly expanding system.

The dynamical process for the formation of nuclei in relativistic heavy-ion collisions is studied and compared with those encountered in a big bang model of nucleosynthesis. It is shown that the scale change in the time coordinate between the two pictures is not compensated by the corresponding scale change in the position coordinate or density so that the details of the nature of the reactions are quite different in the two cases. Moreover, within the framework of the model presented, it is found that reaction rates may initially be fast compared with expansion time scales. If so, a thermodynamic equilibrium will be established for a brief period of time in the space-time expansion of the system. Then, as a working idealization, we have replaced the complicated space-time evolution of the system with a much simpler one in which the system expands through a set of quasiequilibrium states until a volume or density is reached after which collisions cease. A simple argument is then presented showing that this volume or density for light nuclei may be related to the finite size of the correlated structures of the interacting system which eventually become the stable composite nuclei in the transition to the noninteracting stage.

Next, starting with the assumption that the average behavior of the system of nucleons and nuclei produced in a central collision of two relativistic heavy ions closely approximates a thermodynamic system in equilibrium, the simple and elegant mathematical framework of equilibrium thermodynamics is then used to investigate these col-

lisions. A simplified model is first proposed for which the Gibbs grand canonical partition function is easily evaluated. In this model, interactions are included by imposing the constraints of thermal and chemical equilibrium between nucleons and nuclei in their bound states. The ranges of the interactions are also accounted for by the size of the thermodynamic volume where equilibrium is established. In this equilibrium model, the observed properties of the composite particles reflect a "frozen in" equilibrium distribution of the system.

The predictions of the model are then presented. An important result found is that the space-time evolution of the system can be obtained from the composite particle inclusive cross sections. This information is provided by an advantage of high energy heavy-ion collisions in that a significant fraction of deuterons, tritons, and helium nuclei, along with protons and pions, are seen. The size of the emitting region is then obtained without resorting to any Hanbury-Brown-Twiss correlation measurement, as is necessary in p - p collisions.

Another important prediction of the model is that composite particle cross sections should be characterized by Maxwell-Boltzmann distributions in some rest system. Recent data support this conclusion for light fragments of d , t , ${}^3\text{He}$, and ${}^4\text{He}$. Heavier fragments from Li to F can also be described in terms of such distributions but there appear to be disagreements between various extracted parameters and the interpretation and implications of them.

The effect of attractive correlations, responsible for composite structures, on the equation of state and on the energy-temperature relationship are presented. Also discussed in some detail are the effects of the unbound nuclear states on the properties of the system and its spectrum of particles.

ACKNOWLEDGMENTS

The author would like to thank N. Glendenning, M. Gyulassy, W. Myers, M. Redlich, W. Swiatecki, and M. Weiss for many suggestions and the experimentalists of Ref. 5 also for helpful discussions. This work was done under the auspices of the U.S. Energy Research and Development Administration and the National Science Foundation.

APPENDIX A

1. Thermodynamic expressions with relativity and statistics

The basic thermodynamic properties of a system, including the effects of relativity and statistics, are summarized here. The grand canonical partition function for particles obeying Bose-

Einstein statistics (pions, deuterons, α particles) is

$$\mathfrak{Z}_{\text{BE}} = \pi_i \frac{1}{1 - Z e^{-\beta \epsilon_i}}, \quad (\text{A1})$$

and for particles obeying Fermi-Dirac statistics (protons, neutrons, tritons, ${}^3\text{He}$) is

$$\mathfrak{Z}_{\text{FD}} = \pi_i (1 + Z e^{-\beta \epsilon_i}). \quad (\text{A2})$$

The i runs over all quantum states. The $Z = e^{\beta \mu}$, where μ is the chemical potential and $\beta = 1/kT$. The energy $\epsilon_i = (P_i^2 C^2 + M^2 C^4)^{1/2}$. From \mathfrak{Z} all thermodynamic properties follow.

The mean number of particles in state i is given by the well known expressions

$$\langle n_i \rangle = \frac{1}{\exp[(\epsilon_i - \mu)/kT] \pm 1} \quad (\text{A3})$$

with the plus sign for Fermi-Dirac statistics and the minus sign for Bose-Einstein statistics. The number of states in an element of phase space is

$$d^3 \Gamma_{\text{phase-space}} = \frac{V d^3 p}{h^3} (2S + 1). \quad (\text{A4})$$

The density can then be written as

$$\frac{N}{V} = \frac{2S+1}{2\pi^2 \hbar^3} M^2 C kT \times \sum_n \frac{(\pm)^{n+1}}{n} e^{n(\mu/kT)} K_2 \left(n \frac{Mc^2}{kT} \right), \quad (\text{A5})$$

with the minus sign now for Fermi-Dirac particles and the plus sign for Bose-Einstein particles. The K is a modified Bessel function. The equation of state follows from $PV = kT \ln \mathfrak{Z}$ and is therefore

$$PV = \frac{2S+1}{2\pi^2 \hbar^3} VM^2 C (kT)^2 \times \sum_n \frac{(\mp)^{n+1}}{n^2} e^{n(\mu/kT)} K_2 \left(n \frac{Mc^2}{kT} \right). \quad (\text{A6})$$

Similarly, the mean energy E is derived from $-\partial \ln \mathfrak{Z} / \partial \beta$ and is

$$E = \frac{2S+1}{2\pi^2 \hbar^3} VM^3 C^3 kT \times \sum_n \frac{(\mp)^{n+1}}{n} e^{n(\mu/kT)} \left(\frac{3}{4} K_3 + \frac{1}{4} K_1 \right). \quad (\text{A7})$$

The E , here, includes the rest mass energy NMc^2 . The Bessel functions have the same argument as in Eq. (A6). Finally, the entropy S follows from $S = (E + PV - \mu N)/T$. The sum over n gives the corrections due to statistics, and the presence of Bessel functions in the expressions are a result of the relativistic energy-momentum relationship. While the above relationships are exact, they are only useful when the degree of de-

generacy is low (high temperature, low density) so that the sums appearing in Eqs. (A5)–(A7) converge quickly. Various limiting cases are of interest and will now be summarized.

2. Nonrelativistic but with statistics

The nonrelativistic limit of the above equations is obtained in the approximation $\xi = nMc^2/kT \rightarrow \infty$. In this limit the Bessel function has the following asymptotic expansion:

$$K_\nu(\xi) \sim \left(\frac{\pi}{2\xi}\right)^{1/2} e^{-\xi} \times \left(1 + \frac{\gamma-1}{8\xi} + \frac{(\gamma-1)(\gamma-9)}{2!(8\xi)^2} + \dots\right), \quad (\text{A8})$$

where $\gamma = 4\nu^2$. In this limit, the thermodynamic properties for a Fermi-Dirac gas are as follows. For the density:

$$\frac{N}{V} = (2S+1) \frac{1}{\lambda_T^3} f_{3/2}, \quad (\text{A9})$$

where

$$f_{3/2} = \sum_n (-1)^{n+1} \frac{Z^n}{n^{3/2}}, \quad (\text{A10})$$

with $Z = e^{\beta\tilde{\mu}}$, $\tilde{\mu} = \mu - Mc^2$ and $\lambda_T^3 = h^3/(2\pi M kT)^{3/2}$. For the mean energy:

$$E = (2S+1) \frac{V}{\lambda_T^3} \frac{3}{2} kT f_{5/2} + NMc^2, \quad (\text{A11})$$

with

$$f_{5/2} = \sum_n (-1)^{n+1} \frac{Z^n}{n^{5/2}}. \quad (\text{A12})$$

The equation of state is simply related to the energy:

$$PV = \frac{2}{3} (E - NMc^2). \quad (\text{A13})$$

The corresponding results for Bose-Einstein particles are obtainable from Eqs. (A9), (A10), and (A13) when the f_m is replaced by g_m where

$$g_m = \sum_n \frac{Z^n}{n^m}. \quad (\text{A14})$$

3. Nonrelativistic and with expansion in nondegeneracy

When the f_m and g_m are expanded in terms of Z , the lowest order corrections due to statistics follow. Specifically, for Fermi-Dirac particles

$$\frac{N}{V} = \rho = \frac{(2S+1)}{\lambda_T^3} \left(Z - \frac{Z^2}{2^{3/2}} + \frac{Z^3}{3^{3/2}} - \dots \right). \quad (\text{A15})$$

Working to order Z^2 , the above equation can be solved for Z in terms of ρ :

$$Z = \frac{\rho \lambda_T^3}{2S+1} + \frac{1}{2\sqrt{2}} \left(\frac{\rho \lambda_T^3}{2S+1} \right)^2. \quad (\text{A16})$$

The first order correction to the equation of state is then

$$\frac{P}{kT} = \rho \left(1 \pm \frac{1}{2^{5/2}} \frac{\rho \lambda_T^3}{2S+1} \dots \right), \quad (\text{A17})$$

with the plus sign for Fermi-Dirac particles which “repel” each other and increase the pressure and the minus sign for Bose-Einstein particles which “attract” each other and lower the pressure. For the densities and temperatures of interest $\rho \sim \frac{1}{3}$ nuclear matter and $kT \sim 50$ MeV, the second term is $\sim 3\%$ of the first for spin $\frac{1}{2}$ fermions, $\sim 6\%$ of the leading term for spin 0 bosons, and 2% for spin 1 bosons. The corrections to the energy follow from Eqs. (A13) and (A17) and are thus also small. However, doubling the density and reducing the temperature by 2 would multiply these percentages by a factor of 5.6.

4. Ultrarelativistic limit with statistics

The thermodynamic properties in the ultrarelativistic limit with the effects of statistics included are easily derived from the following limit of the Bessel functions:

$$K_\nu(\xi) \rightarrow \frac{\frac{1}{2}\Gamma(\nu)}{\left(\frac{1}{2}\xi\right)^\nu}, \quad \xi \rightarrow 0, \quad (\text{A18})$$

where $\Gamma(\nu) = (\nu-1)!$. Specifically, the density follows from

$$\rho = \frac{2S+1}{\pi^2(\hbar c)^3} (kT)^3 \sum_n (\mp)^{n+1} \frac{e^{n(\mu/kT)}}{n^3}, \quad (\text{A19})$$

while the energy is

$$E = 6 \frac{(2S+1)}{2\pi^2(\hbar c)^3} V(kT)^4 \sum_n \frac{(\mp)^{n+1}}{n^4} e^{n(\mu/kT)}. \quad (\text{A20})$$

The pressure is simply related to the energy density by $P = E/3V$. The above equations reduce to well known results when $\mu = 0$. For massive particles, the ultrarelativistic limit has not been reached and may never be reached if the temperature is limited at $kT \sim 160$ MeV.³⁰

- ¹D. E. Greiner, P. J. Lindstrom, H. H. Heckman, B. Cork, and F. S. Bieser, *Phys. Rev. Lett.* **35**, 152 (1975).
- ²H. H. Heckman, D. E. Greiner, P. J. Lindstrom, and D. D. Tuttle, LBL Report, 1976 (unpublished).
- ³J. Papp, J. Jaros, L. Schroeder, J. Staples, H. Steiner, A. Wagner, and J. Wiss, *Phys. Rev. Lett.* **34**, 601 (1975).
- ⁴G. F. Chapline, M. H. Johnson, E. Teller, and M. S. Weiss, *Phys. Rev. D* **8**, 4302 (1973).
- ⁵J. Gosset, H. H. Gutbrod, W. G. Meyer, A. M. Poskanzer, A. Sandoval, R. Stock, and G. D. Westfall, *Phys. Rev. C* **16**, 629 (1977).
- ⁶G. D. Westfall, J. Gosset, P. J. Johansen, A. M. Poskanzer, W. G. Meyer, H. H. Gutbrod, A. Sandoval, and R. Stock, *Phys. Rev. Lett.* **37**, 1202 (1976).
- ⁷H. Gutbrod, A. Sandoval, P. Johansen, A. Poskanzer, J. Gosset, W. Meyer, G. Westfall, and R. Stock, *Phys. Rev. Lett.* **37**, 667 (1976).
- ⁸J. Stevenson, P. B. Price, and K. Frankel, *Phys. Rev. Lett.* **38**, 1125 (1977).
- ⁹M. Sobel, P. J. Siemens, J. P. Bondorf, and H. A. Bethe, *Nucl. Phys.* **A251**, 502 (1975).
- ¹⁰A. Mekjian, *Phys. Rev. Lett.* **38**, 604 (1977).
- ¹¹See, for example, P. E. Peebles, *Physical Cosmology*, Princeton Series in Physics (Princeton U.P., Princeton, N.J., 1971).
- ¹²S. Weinberg, *Gravitation and Cosmology, Principles and Applications of the General Theory of Relativity* (Wiley, New York, 1972).
- ¹³R. Wagoner, W. A. Fowler, and F. Hoyle, *Astrophys. J.* **148**, 3 (1967); W. A. Fowler and F. Hoyle, *Nucleosynthesis in Massive Stars and Supernovae* (The Univ. of Chicago Press, Chicago, 1965).
- ¹⁴W. J. Swiatecki, LBL report, 1976 (unpublished).
- ¹⁵J. N. Ginocchio (unpublished).
- ¹⁶M. Danos and K. Smith (unpublished).
- ¹⁷Z. Fraenkel and Y. Yariv (unpublished).
- ¹⁸A. A. Amsden, G. F. Bertsch, F. H. Harlow, and J. R. Nix, *Phys. Rev. Lett.* **35**, 905 (1975).
- ¹⁹J. P. Bondorf, H. T. Feldmeier, S. Garpman, and E. C. Halbert, *Phys. Lett.* **65B**, 217 (1976).
- ²⁰A. R. Bodmer and C. N. Panos, *Phys. Rev. C* **15**, 1342 (1977).
- ²¹L. Wilts, R. Chestnut, and Y. Yariv (unpublished).
- ²²C. Kittel, *Elementary Statistical Physics* (Wiley, New York, 1958), Appendix C, p. 219, discusses the approach to thermal equilibrium of 100 hard sphere particles in a box. Starting from a highly nonthermal distribution, a Maxwell-Boltzmann distribution is approximately established after only three collisions per particle.
- ²³V. Ruck, M. Gyulassy, and W. Greiner, *Z. Phys.* **A277**, 391 (1976), discuss a novel mechanism for thermalization through an enhancement in the scattering of nucleons via a collective field.
- ²⁴An equilibrium process has been introduced in Ref. 13 as a mechanism for accounting for the abundances of the iron group of elements generated in supernova stars. Equilibrium distributions also characterize the early periods of the expansion of an isotropic and homogeneous universe, and at later stages in this expansion, the production of deuterium through $n + p \rightarrow d + \gamma$ is fast enough for deuterium to achieve its equilibrium concentration (Refs. 11–13).
- ²⁵G. Gamow, *Nature* **162**, 680 (1948).
- ²⁶The reciprocal of this reaction rate (10^{-19} sec) would be a characteristic time scale for black-body radiation to develop at a temperature $kT = 50$ MeV through absorption and emission of radiation from giant resonances of the nuclear components. An indicator of a very long-lived system, 10^3 – 10^4 times longer than what is naively expected on very simple grounds, would be the presence of black-body radiation at a temperature of $kT = 50$ MeV.
- ²⁷M. Davidson *et al.*, *Phys. Lett.* **3**, 358 (1963).
- ²⁸V. Lyons *et al.*, *Phys. Lett.* **3**, 359 (1963).
- ²⁹J. Kapusta, *Phys. Rev. C* **15**, 1580 (1977).
- ³⁰R. Hagedorn, *Cargèse Lectures in Physics*, edited by E. Schatzman (Gordon and Breach, New York, 1973), Vol. 6, p. 643.
- ³¹R. Hanbury-Brown and R. Q. Twiss, *Nature (London)* **178**, 1046 (1956).
- ³²G. Goldhaber, S. Goldhaber, W. Yee, and A. Pais, *Phys. Rev.* **120**, 300 (1960).
- ³³G. I. Kopylov, *Phys. Lett.* **50B**, 472 (1974).
- ³⁴C. Ezell, L. J. Gutay, A. T. Laasanen, F. I. Dao, P. Schübenlin, and F. Turkot, *Phys. Rev. Lett.* **38**, 873 (1977).
- ³⁵S. T. Butler and C. A. Pearson, *Phys. Rev.* **129**, 836 (1963).
- ³⁶A. Schwarzschild and C. A. Pearson, *Phys. Rev.* **129**, 854 (1963).
- ³⁷E. Beth and G. E. Uhlenbeck, *Physica* **4**, 915 (1937).
- ³⁸S. Z. Belenky, *Nucl. Phys.* **2**, 259 (1956).
- ³⁹E. Fermi, *Prog. Theor. Phys.* **5**, 570 (1950).
- ⁴⁰K. M. McVoy, *Ann. Phys. (N.Y.)* **43**, 91 (1967).
- ⁴¹N. Levinson, K. Dan. Vidensk. Selsk., *Mat-Fys. Medd.* **25**, No. 9 (1949).
- ⁴²E. P. Wigner, *Phys. Rev.* **98**, 145 (1955).
- ⁴³E. E. Salpeter, *Astrophys. J.* **115**, 326 (1952); F. Hoyle, *Astrophys. J. Suppl.* **1**, 121 (1954).
- ⁴⁴A. Bohr and B. Mottleson, *Nuclear Structure, I. Single-Particle Motion* (Benjamin, New York, 1969).
- ⁴⁵In a thermodynamic approach to atomic systems, the partition function diverges if all the levels are included in the state sum. However, the divergence comes from the levels near zero energy for which the electronic orbitals have increasing dimensions. Since the composite structure of an atom is bounded by neighboring atoms, the state sum is to be limited in order for a thermodynamic description to make sense. See E. Fermi, *Z. Phys.* **26**, 54 (1924).
- ⁴⁶S. Fiarman and S. S. Hanna, *Nucl. Phys.* **A251**, 1 (1975).
- ⁴⁷S. Fiarman and W. E. Meyerhof, *Nucl. Phys.* **A206**, 1 (1973).
- ⁴⁸F. Ajzenberg-Selove and T. Lauritsen, *Nucl. Phys.* **A227**, 1 (1974).
- ⁴⁹G. I. Kopylov and M. I. Podgoretskii, *Sov. J. Nucl. Phys.* **15**, 392 (1972).
- ⁵⁰S. E. Koonin, *Phys. Lett.* **70B**, 43 (1977).